Article:

Li, Q. orcid.org/0000-0003-2503-690X, Huang, L. orcid.org/0000-0003-4534-7625, Liu, W. orcid.org/0000-0003-2968-2888 et al. (2 more authors) (2023) Cold-start satellite signal acquisition aided by an antenna array in the presence of outliers. IEEE Transactions on Vehicular Technology, 72 (5). pp. 5847-5861. ISSN 0018-9545

https://doi.org/10.1109/tvt.2022.3230543

Acquisition of Visible Satellites Based on Antenna Arrays via Joint $\ell_{1,1}$-Norms Minimization

Qiang Li, Lei Huang, *Senior Member, IEEE*, Wei Liu, *Senior Member, IEEE*, Lifang Feng, Xinzhu Chen

***Abstract*—This work tackles the acquisition of visible satellites based on an antenna array in the presence of impulsive noise. First, the joint angle and number estimation of visible satellites is formulated as a joint $\ell_{1,1}$-norms minimization problem by exploiting the spatial sparsity of visible satellites. Then, in order to obtain a closed-form solution, a generalized conjugate function for complex-valued matrix variable is introduced and the joint $\ell_{1,1}$-norms minimization is transformed into a Lagrangian dual function maximization. Furthermore, the dual ascent framework and subgradient technique are employed to obtain a suitable iterative solution, where the convergence rate and steady-state value can be flexibly adjusted. Numerical results are presented to demonstrate the effectiveness of the proposed approach.**

***Index Terms*—Antenna arrays, acquisition of visible satellites, Lagrangian multiplier, dual ascent, impulsive noise, $\ell_{1,1}$-norm.**

I. Introduction

ACQUISITION of satellite signals is a three-dimensional (3-D) search process including visible satellite, Doppler frequency and pseudorandom noise (PRN) code phase [1]. Normally, the joint angle and number estimation (JANE) of visible satellites should be performed first for the quick selection of satellite geometrical dilution of precision (GDOP) [2]. Moreover, the determination of visible satellites directly affects the time consumption and success probability of the search in the other two-dimensions.

For the traditional navigation receiver with a single antenna, the determination of visible satellites requires some prior information, such as satellite ephemeris or almanac, general location of receiver. However, the information can only be extracted after baseband signal processing is completed. Especially for a satellite receiver working in the cold-start mode without assistance of satellite ephemeris or almanac, the receiver has to perform a time-consuming blind 3-D search [2].

Antenna arrays can sense signal impinging angle and suppress interference, and therefore a satellite receiver with antenna arrays has excellent potential to determine the JANE of visible satellites in the presence of impulsive noise [3]. There is an extensive literature about angle estimation using antenna arrays at the stage of signal tracking, where the number of satellite signals is normally assumed to be known [4]. To the best of our knowledge, in the presence of impulsive noise, the research on JANE of visible satellites via an antenna array at the stage of acquisition has not yet received much attention.

Motivated by compressed sensing (CS) theory [5] and spatial sparsity of visible satellites that only 6-12 satellites can be observed normally [2], the acquisition of visible satellites is considered from the viewpoint of row-sparse or low-rank matrix recovery [6]. One popular method called low-rank matrix approximation (LRMA) [7] is applied to recover a low-rank matrix, where additive white Gaussian noise is assumed and a soft-threshold function [8] needs to be carefully designed. However, the singular value thresholding (SVT) technique in the LRMA tends to underestimate nonzero singular values [6], which makes it difficult to select a suitable soft-threshold function. In addition, numerous methods have been developed to solve the problem of sparse matrix recovery, such as orthogonal least squares [9], Hankel matrix completion [10] and iterative reweighted rank minimization [11]. Generally, these methods perform well in the case of Gaussian noise while the performance may degrade significantly in the presence of impulsive noise.

In order to tackle the issue, some optimization methods using principal component analysis (PCA) technique [12] and $\ell_{2,p}$-norm framework [13]–[15] have been proposed. Considering that some columns of a matrix are arbitrarily corrupted, a robust PCA method that minimizes the nuclear norm and $\ell_{2,1}$-norm loss function is developed to suppress outliers [12]. By employing joint $\ell_{2,1}$-norms minimization on both loss function and regularization, a robust and efficient method is proposed for feature selection [14], where the loss function is robust to outliers. More generally, using the row sparse structure, a cost function for angle estimation with general $\ell_{2,p}$-norm $(0 < p \leq 1)$ is proposed in [15], where the choice of p is related to the statistical properties of noise.

Inspired by the joint $\ell_{2,1}$-norms framework and spatial sparsity of visual satellites, the JANE of visible satellites in the presence of impulsive noise is formulated as a joint $\ell_{1,1}$-norms optimization, which has more robust ability to suppress impulsive noise than that of the $\ell_{2,1}$-norm. To avoid using

This work was supported in part by Shenzhen Stabilization Support under Grant 20200809153412001, in part by Guangdong Basic and Applied Basic Research Foundation under Grants 2021A1515011855, 2019A1515110509, in part by the National Natural Science Foundation of China under Grants 61801302, 62101347, 62101345, in part by the National Science Fund for Distinguished Young Scholars under Grant 61925108, in part by the Key Project of International Cooperation and Exchanges of the National Natural Science Foundation of China under Grant 62220106009, and in part by Foundation of China Postdoctoral Science under Grant 2021M702274. The review of this article was coordinated by ***. *(Corresponding authors: Lifang Feng; Lei Huang.)*

Qiang Li, Lei Huang, Lifang Feng, and Xinzhu Chen are with the College of Electronics and Information Engineering, Shenzhen University, Shenzhen 518060, China (e-mail: liqiang198780@163.com; lhuang@szu.edu.cn).

Wei Liu is with the Department of Electronic and Electrical Engineering, University of Sheffield, Sheffield S10 2TN, U.K. (e-mail: w.liu@sheffield.ac.uk).

Digital Object Identifier ***

time-consuming CVX optimization tool [16], the Lagrangian dual function is devised by employing a generalized conjugate function for complex-valued matrix. In addition, the dual ascent framework and the subgradient technique are applied to obtain an iterative closed-form solution.

Notations: In the paper, bold lowercase letter and bold uppercase letter denote vector and matrix, respectively. $\mathbb{R}$ and $\mathbb{C}$ are real-valued set and complex-valued set, respectively. $(\cdot)^T$, $(\cdot)^*$, $(\cdot)^H$, $|\cdot|$, $\mathrm{Tr}(\cdot)$ and $\odot$ represent transpose, conjugate, conjugate transpose, absolute value, trace and Hadamard product, respectively. x_{ij} represents the (i,j)-th entry of a matrix $\boldsymbol{X}$. $f:\mathbb{R}^{m\times n}\rightarrow\mathbb{R}^{p\times q}$ stands for that f is an $\mathbb{R}^{p\times q}$-valued function on some subsets of $\mathbb{R}^{m\times n}$ and the domain of function f is denoted as $\mathbf{dom}f$. "sup" and "inf" represent the supremum and infimum of a function, respectively. $\|\boldsymbol{X}\|_{r,p}$ is the $\ell_{r,p}$-norm [13], defined as

$$\|\boldsymbol{X}\|_{r,p}=\left[\sum_{i=1}^{m}\left(\sum_{j=1}^{n}|x_{ij}|^{r}\right)^{\frac{p}{r}}\right]^{\frac{1}{p}}, \tag{1}$$

where $\ell_{1,1}$-norm is a special case of the $\ell_{r,p}$-norm.

II. Problem Formulation

Consider Q visible satellite signals impinging on a uniform linear array (ULA) consisting of M antenna elements with inter-element spacing d. After down conversion, sampling and quantization [2], the satellite signals arriving at the m-th antenna element can be expressed as

$$y_m(t)=\sum_{q=1}^{Q}x_q(t)e^{j2\pi(m-1)\sin(\theta_q)d/\lambda}+n_m(t), \tag{2}$$

where t represents the sampling time, λ is the carrier wavelength of the satellite signal, θ_q is the direction of arrival (DOA) of the q-th signal, $n_m(t)$ denotes the noise at the m-th element and $x_q(t)$ represents the q-th satellite signal, i.e.,

$$x_q(t)=\sqrt{2p_q}D_q(t)C_q(t)e^{j(2\pi f_{IF}^{q}t+\phi_0^{q})}, \tag{3}$$

where p is the signal power, D stands for the bit stream of the navigation data with uncertain symbol ±1, C denotes the spreading PRN code sequence, f_{IF} is the signal intermediate frequency (IF) and ϕ_0 is the initial phase.

Normally, the number of visual satellites Q is unknown before acquisition process is completed. However, according to the prior information of satellite ephemeris or almanac, the approximate angle region of visible satellites is known. Therefore, by arranging the incident signals at antenna arrays in a vector $\boldsymbol{y}(t)=[y_1(t),\cdots,y_M(t)]^T$, the received signals model (2) can be written in a more compact form

$$\boldsymbol{y}(t)=\boldsymbol{A}\boldsymbol{x}(t)+\boldsymbol{n}(t), \tag{4}$$

where $\boldsymbol{x}(t)\in\mathbb{C}^{L\times1}$ is a sparse vector with only $Q(Q<L)$ satellite signals and $\boldsymbol{A}\in\mathbb{C}^{M\times L}$ denotes array manifold matrix which is of the form

$$\boldsymbol{A}=[\boldsymbol{a}(\theta_1),\boldsymbol{a}(\theta_2),\cdots,\boldsymbol{a}(\theta_L)] \tag{5}$$

with $\boldsymbol{a}(\theta)$ being the steering vector

$$\boldsymbol{a}(\theta)=\left[1,e^{j2\pi\frac{d\sin\theta}{\lambda}},\cdots,e^{j2\pi(M-1)\frac{d\sin\theta}{\lambda}}\right]^T,\quad\theta\in\boldsymbol{\Theta}, \tag{6}$$

where $\boldsymbol{\Theta}$ is the angle region of interest, which is uniformly discretized into L angles in (5).

Then, assuming that the number of samples in temporal domain is N, the matrix formulation of (4) can be written as

$$\boldsymbol{Y}=\boldsymbol{A}\boldsymbol{X}+\boldsymbol{N}, \tag{7}$$

where $\boldsymbol{Y}=[\boldsymbol{y}(1),\cdots,\boldsymbol{y}(N)]\in\mathbb{C}^{M\times N}$ and $\boldsymbol{X}\in\mathbb{C}^{L\times N}$ has row sparsity, where only Q rows have non-zero elements. Obviously, the JANE of satellite signals can be completed if the non-zero rows in $\boldsymbol{X}$ are estimated accurately.

III. Proposed Algorithm

A. Proposed Optimization Model and Analysis

In (7), if the noise follows Gaussian distribution, many state-of-the-art algorithms can effectively tackle the JANE problem. However, their performance may degrade significantly in the presence impulsive noise. We know that a joint $\ell_{2,1}$-norms minimization framework on both loss function and regularization is efficient and robust for feature selection in the presence of outliers [14], which motivates us to study the JANE problem using the framework of joint $\ell_{1,1}$-norms minimization. To be specific, the optimization model is formulated as

$$\min_{\boldsymbol{X}}\quad\left\{f(\boldsymbol{X})=\|\boldsymbol{Y}-\boldsymbol{A}\boldsymbol{X}\|_{1,1}+\gamma\|\boldsymbol{X}\|_{1,1}\right\}, \tag{8}$$

where $\|\boldsymbol{Y}-\boldsymbol{A}\boldsymbol{X}\|_{1,1}$ is used to effectively suppress the effect of impulsive noise and $\|\boldsymbol{X}\|_{1,1}$ can approximate the concave $\|\boldsymbol{X}\|_{1,0}$ to enforce a row sparse solution. Furthermore, by varying the regularization factor γ, we can sweep out the optimal trade-off value between $\|\boldsymbol{Y}-\boldsymbol{A}\boldsymbol{X}\|_{1,1}$ and $\|\boldsymbol{X}\|_{1,1}$. Actually, for the optimization (8), the proposed joint $\ell_{1,1}$-norms model has more robust ability to suppress outliers than that of the joint $\ell_{2,1}$-norms model [14], which will be verified in the simulation section later.

B. Discussion and Analysis on Solving Method

The objective function (8) is convex [14] and the CVX optimization tool [16] can be employed to solve the problem, which is called "CVX-$\ell_{1,1}$-norm" herein. However, the interior point technique [16] is used in the CVX optimization, which cannot get a closed-form solution and it is also unfriendly to computational complexity.

Furthermore, the subgradient technique [17], [18] can easily be thought of to solve this optimization problem (8). In particular, according to the **Lemmas 1-2**, the conjugate subgradient of $f(\boldsymbol{X})$ in (8) with respect to $\boldsymbol{X}^*$ can be formulated as

$$\nabla_{\mathbf{X}^*}f(\boldsymbol{X})=\frac{\partial f(\boldsymbol{X})}{\partial\boldsymbol{X}^*}=\frac{1}{2}\boldsymbol{A}^H[\boldsymbol{H}\odot(\boldsymbol{A}\boldsymbol{X}-\boldsymbol{Y})]+\frac{\gamma}{2}\boldsymbol{R}\odot\boldsymbol{X}, \tag{9}$$

where $\boldsymbol{H}$ and $\boldsymbol{R}$ are given in detail in the **Lemmas 1-2**. Note that each update of the variable $\boldsymbol{X}$ by the subgradient technique does not guarantee that the cost function $f(\boldsymbol{X})$ is monotonically decreasing. In addition, it is not easy to determine the update step size [17].

Lemma 1: For a complex-valued matrix $\boldsymbol{X} \in \mathbb{C}^{L\times N}$, taking the conjugate subgradient of $\|\boldsymbol{X}\|_{1,1}$ with respect to $\boldsymbol{X}^*$, leads to

$$\frac{\partial\|\boldsymbol{X}\|_{1,1}}{\partial\boldsymbol{X}^*} = \frac{\partial\sum_{i=1}^{L}\sum_{j=1}^{N}\left(x_{i,j}^*x_{i,j}\right)^{\frac{1}{2}}}{\partial\boldsymbol{X}^*} = \frac{1}{2}\boldsymbol{R}\odot\boldsymbol{X}, \quad (10)$$

where the element $x_{i,j}$ is assumed to be non-zero valued here and $\boldsymbol{R} \in \mathbb{R}^{L\times N}$ is a real-valued matrix with the (i,j)-th element being $r_{i,j} = 1/|x_{i,j}|$.

Lemma 2: A complex-valued matrix $\boldsymbol{W} \in \mathbb{C}^{M\times N}$ has the form $\boldsymbol{W} = \boldsymbol{A}\boldsymbol{X}$ with $\boldsymbol{A} \in \mathbb{C}^{M\times L}$ and $\boldsymbol{X} \in \mathbb{C}^{L\times N}$. According to the definition of $\ell_{1,1}$-norm in (1), we have

$$\|\boldsymbol{W}\|_{1,1}=\sum_{i=1}^{M}\sum_{j=1}^{N}\sqrt{w_{i,j}w_{i,j}^*}=\sum_{i=1}^{M}\sum_{j=1}^{N}\sqrt{w_{i,j}\left(\sum_{l=1}^{L}a_{i,l}^*x_{l,j}^*\right)}. \quad (11)$$

Taking the subgradient of $\|\boldsymbol{W}\|_{1,1}$ with respect to $\boldsymbol{X}^*$, the result can be written as

$$\frac{\partial\|\boldsymbol{W}\|_{1,1}}{\partial\boldsymbol{X}^*}=\frac{1}{2}\begin{bmatrix}\sum_{i=1}^{M}\frac{w_{i,1}a_{i,1}^*}{|w_{i,1}|} & \cdots & \sum_{i=1}^{M}\frac{w_{i,N}a_{i,1}^*}{|w_{i,N}|}\\ \vdots & \ddots & \vdots\\ \sum_{i=1}^{M}\frac{w_{i,1}a_{i,L}^*}{|w_{i,1}|} & \cdots & \sum_{i=1}^{M}\frac{w_{i,N}a_{i,L}^*}{|w_{i,N}|}\end{bmatrix}. \quad (12)$$

Furthermore, define $\boldsymbol{H} \in \mathbb{R}^{M\times N}$ as a real-valued matrix with the (i,j)-th element being $h_{i,j} = 1/|w_{i,j}|$. A simplified expression of (12) is given by

$$\frac{\partial\|\boldsymbol{W}\|_{1,1}}{\partial\boldsymbol{X}^*} = \frac{1}{2}\boldsymbol{A}^H\left(\boldsymbol{H}\odot\boldsymbol{W}\right) = \frac{1}{2}\boldsymbol{A}^H[\boldsymbol{H}\odot(\boldsymbol{A}\boldsymbol{X})]. \quad (13)$$

In the following sections, we try to solve the optimization (8) and get an iterative closed-form solution by devising a cost function of the Lagrangian dual optimization and applying the dual ascent technique [17].

C. Proposed Dual Lagrangian Model

As an unconstrained optimization problem, the optimization problem (8) can be further reformulated as

$$\min_{\boldsymbol{X},\boldsymbol{E}} \quad \|\boldsymbol{E}\|_{1,1} + \|\boldsymbol{X}\|_{1,1} \quad \text{s.t.} \quad \boldsymbol{Y} - \boldsymbol{A}\boldsymbol{X} = \gamma\boldsymbol{E}, \quad (14)$$

where $\boldsymbol{E} = (\boldsymbol{Y} - \boldsymbol{A}\boldsymbol{X})/\gamma$. Furthermore, after simple rearrangement, it is easy to get

$$\min_{\boldsymbol{X},\mathbf{E}} \quad \left\|\begin{bmatrix}\boldsymbol{X}\\ \boldsymbol{E}\end{bmatrix}\right\|_{1,1} \quad \text{s.t.} \quad \begin{bmatrix}\boldsymbol{A}, & \gamma\boldsymbol{I}\end{bmatrix}\begin{bmatrix}\boldsymbol{X}\\ \boldsymbol{E}\end{bmatrix} = \mathbf{Y}, \quad (15)$$

where $\mathbf{I} \in \mathbb{R}^{M\times M}$ is an identity matrix.

For notational simplicity, denote $\boldsymbol{Z} = [\boldsymbol{X}^T, \boldsymbol{E}^T]^T \in \mathbb{C}^{P\times N}$, $P = L + M$ and $\boldsymbol{B} = [\boldsymbol{A}, \gamma\boldsymbol{I}] \in \mathbb{C}^{M\times P}$. Consequently, a concise optimization problem with constraint is formulated as

$$\min_{\boldsymbol{Z}} \quad f(\boldsymbol{Z}) \quad \text{s.t.} \quad \boldsymbol{B}\boldsymbol{Z} = \boldsymbol{Y}, \quad (16)$$

where $f(\boldsymbol{Z}) = \|\boldsymbol{Z}\|_{1,1}$.

After that, the Lagrangian multiplier method is used to transform the above problem into an unconstrained minimization problem with the cost function

$$\mathcal{L}(\boldsymbol{Z},\boldsymbol{\Lambda}) = f(\boldsymbol{Z}) + \mathrm{Tr}\left[\boldsymbol{\Lambda}(\boldsymbol{B}\boldsymbol{Z}-\boldsymbol{Y})^H\right], \quad (17)$$

where $\boldsymbol{\Lambda} \in \mathbb{C}^{M\times N}$ is the Lagrangian multiplier matrix.

Definition 1: In [17], let $f : \mathbb{R}^n \to \mathbb{R}$ and then the conjugate function $f^* : \mathbb{R}^n \to \mathbb{R}$ is defined as

$$f^*(\boldsymbol{y}) = \sup_{\boldsymbol{x}\in\mathbf{dom}f}\left[\boldsymbol{y}^T\boldsymbol{x} - f(\boldsymbol{x})\right], \quad (18)$$

where $\boldsymbol{x}$ and $\boldsymbol{y}$ are real-valued vectors.

On the basis of the above statement, this work generalizes the definition of conjugate function to complex-valued matrix variable. Specifically, let $f : \mathbb{C}^{m\times n} \to \mathbb{C}$ and the generalized conjugate function $f^* : \mathbb{C}^{m\times n} \to \mathbb{C}$ can be expressed as

$$f^*(\boldsymbol{U}) = \sup_{\boldsymbol{X}\in\mathbf{dom}f}\left[\mathrm{Tr}(\boldsymbol{U}\boldsymbol{X}^H) - f(\boldsymbol{X})\right], \quad (19)$$

where $\boldsymbol{U}$ and $\boldsymbol{X}$ are complex-valued matrices.

Then, according to the **Definition 1**, the dual objective function of the optimization (16) can be expressed as

$$\begin{aligned} g(\boldsymbol{\Lambda}) &= \inf_{\boldsymbol{Z}}\left\{f(\boldsymbol{Z}) + \mathrm{Tr}\left[\boldsymbol{\Lambda}(\boldsymbol{B}\boldsymbol{Z}-\boldsymbol{Y})^H\right]\right\}\\ &= -\mathrm{Tr}(\boldsymbol{\Lambda}\boldsymbol{Y}^H) - \sup_{\boldsymbol{Z}}\left\{\mathrm{Tr}\left(-\boldsymbol{\Lambda}\boldsymbol{Z}^H\boldsymbol{B}^H\right) - f(\boldsymbol{Z})\right\}\\ &= -\mathrm{Tr}(\boldsymbol{\Lambda}\boldsymbol{Y}^H) - \sup_{\boldsymbol{Z}}\left\{\mathrm{Tr}\left[(-\boldsymbol{B}^H\boldsymbol{\Lambda})\boldsymbol{Z}^H\right] - f(\boldsymbol{Z})\right\}\\ &= -\mathrm{Tr}(\boldsymbol{\Lambda}\boldsymbol{Y}^H) - f^*(-\boldsymbol{B}^H\boldsymbol{\Lambda}) \end{aligned} \quad (20)$$

Therefore, with the help of the conjugate function and Lagrangian multiplier technique, the optimization (16) is transformed into a dual maximization problem, i.e.,

$$\max_{\boldsymbol{\Lambda}} \quad -f^*(-\boldsymbol{B}^H\boldsymbol{\Lambda}) - \mathrm{Tr}(\boldsymbol{\Lambda}\boldsymbol{Y}^H). \quad (21)$$

Furthermore, the objective function $f(\boldsymbol{Z})$ is convex and the constraint is affine function in (16). Therefore, according to the Slater theorem [17], the strong duality condition holds, which indicates that the optimal value of objective function in (16) is the same as that in (21). Therefore, assume that the optimal solution to (21) is $\tilde{\boldsymbol{\Lambda}}$ and then the optimal solution to (16) can be calculated by

$$\tilde{\boldsymbol{Z}} = \arg\min_{\boldsymbol{Z}}\mathcal{L}(\boldsymbol{Z},\tilde{\boldsymbol{\Lambda}}). \quad (22)$$

D. Dual Ascent Method Using Subgradient Technique

Normally, dual ascent method is used to get a suitable solution to (22), where the iterative gradient ascent technique is involved. Specifically, the dual ascent method consists of the following two key steps

$$\boldsymbol{Z}_{k+1} = \arg\min_{\boldsymbol{Z}}\mathcal{L}(\boldsymbol{Z},\boldsymbol{\Lambda}_k), \quad (23)$$

$$\boldsymbol{\Lambda}_{k+1} = \boldsymbol{\Lambda}_k + \mu\nabla_{\boldsymbol{\Lambda}^*}\mathcal{L}(\boldsymbol{Z}_{k+1},\boldsymbol{\Lambda}_k), \quad (24)$$

where k denotes the k-th iteration, the update process (23) is the minimization of the original variable $\boldsymbol{Z}$ and the update process of the dual variable $\boldsymbol{\Lambda}$ is described in (24), with μ being the step size. $\nabla_{\boldsymbol{\Lambda}^*}\mathcal{L}(\boldsymbol{Z},\boldsymbol{\Lambda})$ is the conjugate gradient of the function $\mathcal{L}(\boldsymbol{Z}, \boldsymbol{\Lambda})$ with respect to the conjugate of dual variable $\boldsymbol{\Lambda}$.

Furthermore, in order to obtain the iterative solution to (23) and (24) in closed form, **Lemma 3** should be introduced.

Lemma 3: The trace of matrix has the operation rules [18] as follows.

$$\mathrm{Tr}(\boldsymbol{ABC}) = \mathrm{Tr}(\boldsymbol{CAB}) \tag{25}$$

$$\frac{\partial}{\partial \boldsymbol{X}^*}\mathrm{Tr}(\boldsymbol{A}\boldsymbol{X}^H) = \boldsymbol{A}. \tag{26}$$

According to the **Lemmas 1** and **3** and taking the conjugate subgradient of the function $\mathcal{L}(\boldsymbol{Z})$ in (17) with respect to $\boldsymbol{Z}^*$, it is easy to get

$$\nabla_{\mathbf{Z}^*}\mathcal{L}(\boldsymbol{Z}, \boldsymbol{\Lambda}) = \frac{\partial \mathcal{L}(\boldsymbol{Z}, \boldsymbol{\Lambda})}{\partial \boldsymbol{Z}^*} = \frac{1}{2}\boldsymbol{G} \odot \boldsymbol{Z} + \boldsymbol{B}^H\boldsymbol{\Lambda}, \tag{27}$$

where $\boldsymbol{G} \in \mathbb{R}^{P\times N}$ is a real-valued matrix with the i, j-th element being $g_{i,j} = 1/|z_{i,j}|$.

Therefore, $\boldsymbol{Z}_{k+1}$ in (23) can be updated by

$$\boldsymbol{Z}_{k+1} = \boldsymbol{Z}_k - \frac{\eta}{k+1}\nabla_{\mathbf{Z}^*}\mathcal{L}(\boldsymbol{Z}_k, \boldsymbol{\Lambda}_k). \tag{28}$$

where $\eta/(k+1)$ denotes the step size, which should satisfy the divergent-series rule [17] due to the subgradient operation in (27).

Similarly, taking the conjugate gradient of the function $\mathcal{L}(\boldsymbol{Z})$ with respect to $\boldsymbol{\Lambda}^*$, we have

$$\nabla_{\mathbf{\Lambda}^*}\mathcal{L}(\boldsymbol{Z}, \boldsymbol{\Lambda}) = \frac{\partial \mathcal{L}(\boldsymbol{Z}, \boldsymbol{\Lambda})}{\partial \boldsymbol{\Lambda}^*} = \boldsymbol{BZ} - \boldsymbol{Y}. \tag{29}$$

As mentioned above, to solve (23) and (24), the initial values of $\boldsymbol{Z}$ and $\boldsymbol{\Lambda}$ should be assumed and an iterative framework needs to be applied. After the iteration is completed, the estimation of matrix $\hat{\boldsymbol{X}}$ can be easily extracted from $\boldsymbol{Z}$.

E. Summary of the Proposed Method

To sum up, the optimization (16) is transformed into the Lagrangian dual maximization problem and then the dual ascent technique using iterative framework is employed to find the solution. Note that the JANE of satellite signals is completed if the non-zero rows in the matrix $\hat{\boldsymbol{X}}$ are estimated accurately. For convenience of expression, the above method is called "Lagrangian dual ascent $\ell_{1,1}$-norm (LDA-$\ell_{1,1}$-norm)" algorithm here, which is summarized in the **Algorithm 1**.

Algorithm 1: LDA-$\ell_{1,1}$-norm Algorithm

Input: $M, N, L, Q, K, \boldsymbol{A}, \boldsymbol{Y}, \gamma, \eta, \mu$

Step 1. Initialize $\boldsymbol{Z}_0 \in \mathbb{C}^{P\times N} \leftarrow$ a random matrix, $\boldsymbol{\Lambda}_0 \in \mathbb{R}^{M\times N} \leftarrow$ an all-one matrix.

for $k = 1, 2, \cdots, K$ **do**

Step 2. Determin $\boldsymbol{G}_k$ by $g_{i,j} = 1/|z_{i,j}|$.

Step 3. Calculate $\boldsymbol{Z}_{k+1}$ by (27) and (28).

Step 4. Update $\boldsymbol{\Lambda}_{k+1}$ by (24) and (29).

end for

Output: $\boldsymbol{Z}_K, \hat{\boldsymbol{X}}$.

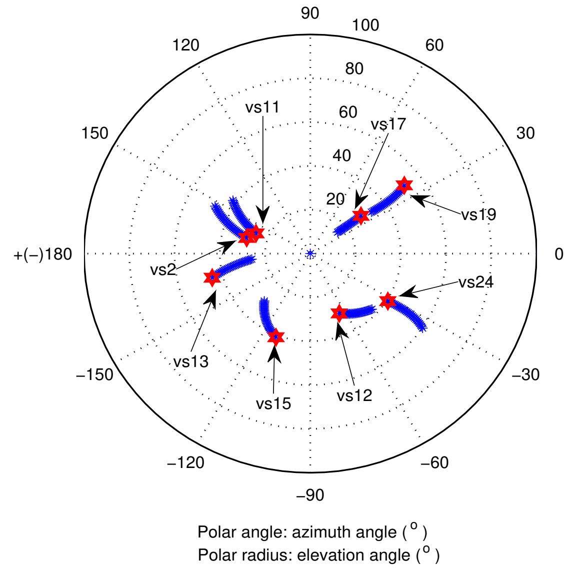

Fig. 1. Angle trajectories of the visible satellites.

F. Complexity Analysis

In this work, the time-consuming calculations are in (24), (27), (28) and (29). Specifically, the analysis is as follows.

1) The complexity of (24) and (29) is $\mathcal{O}(PMN + MN)$, which can be further simplified as $\mathcal{O}(PMN)$.

2) Furthermore, the complexity of (27) and (28) is $\mathcal{O}(PMN + PN)$, which can be further simplified as $\mathcal{O}(PMN)$.

3) In addition, considering the number of iterations K, the total complexity of the proposed algorithm is $\mathcal{O}(KPMN)$, which is determined by the number of iterations K, the parameter L, the number of antennas M and the number of samples N.

IV. Simulation Results

In the simulation, a vehicle is located at Shenzhen University (latitude/longitude: 22.53°N/113.94°E) and the almanac of GPS satellites on 25th June, 2022 is collected [19]. The software-defined GPS receiver [20] is modified by adding an antenna array module, where the satellites whose elevation angles greater than 10° are considered as visible ones and the simulation time is 45 minutes. During the simulation, the azimuth and elevation angles of visible satellites are shown in Fig. 1, where the red pentagrams denote initial azimuth and elevation angles. In the following tests, the 12^{th}, 17^{th}, 19^{th} and 24^{th} satellites are selected. Their initial elevation angles are approximately 30°, 28°, 52° and 40°, respectively.

Then , a ULA consisting of $M = 50$ antennas is used and the elevation region of interest $\boldsymbol{\Theta}$ in (6) is assumed to be $\boldsymbol{\Theta} = [25°, 55°]$, which is uniformly discretized with a step size of 1°, i.e., $L = 31$ in (5). In addition, a two-component Gaussian mixture model (GMM) is used to generate impulsive noise [21], where the proportion component of outliers is 10% and the variances of the two terms are 1 and 50, respectively. The signal-to-noise ratios (SNRs) of satellite

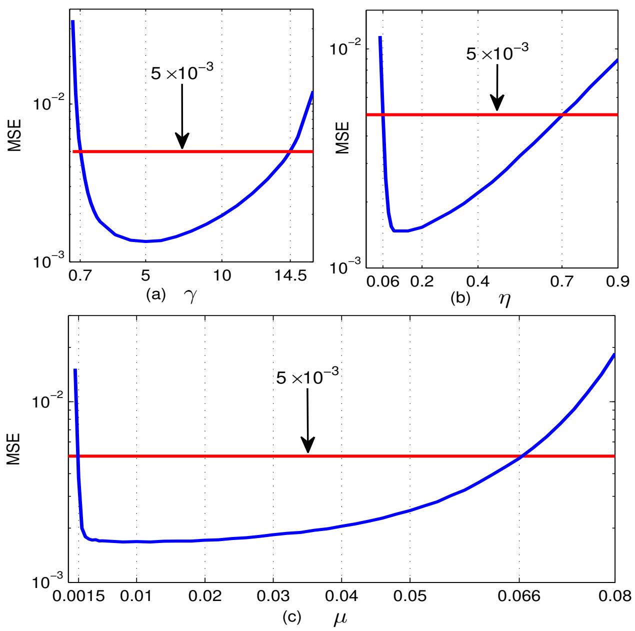

Fig. 2. MSE versus the tunable parameters: (a) regularization factor γ, $\eta = 0.1$, $\mu = 0.01$, (b) step parameter η, $\gamma = 5$, $\mu = 0.01$, (c) step size μ, $\gamma = 5$, $\eta = 0.3$.

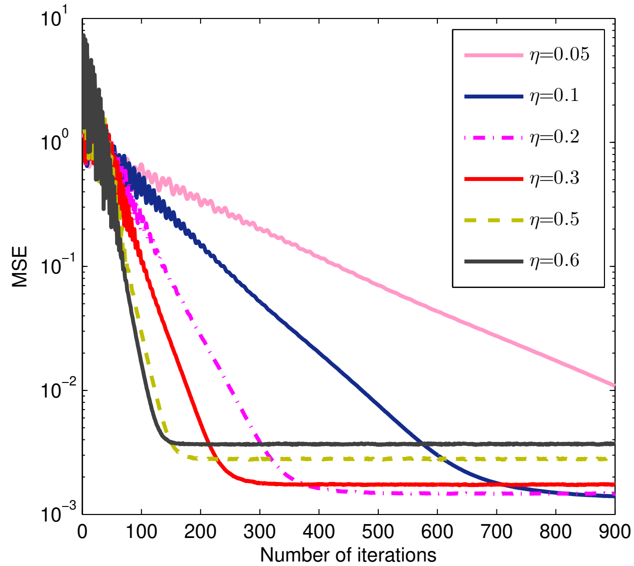

Fig. 3. MSE versus number of iterations, $\gamma = 5$, $\mu = 0.01$.

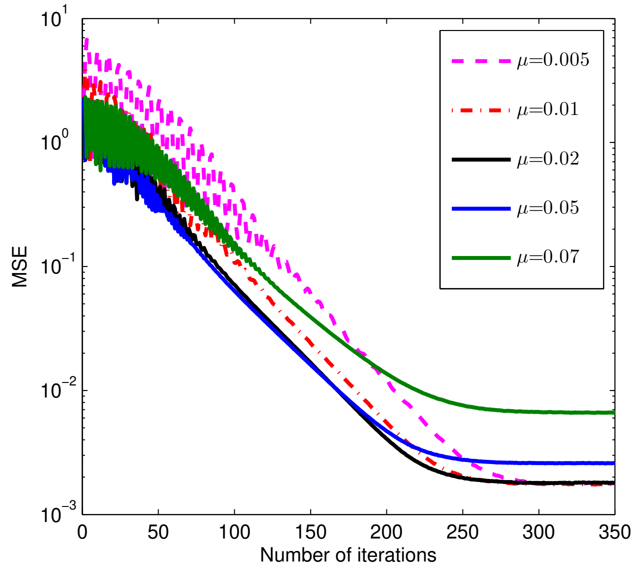

Fig. 4. MSE versus number of iterations, $\gamma = 5$, $\eta = 0.3$.

signals are fixed at 20dB and the snapshot number is 100. Furthermore, initialize $\boldsymbol{Z}_0 \in \mathbb{C}^{P\times N}$ with a random matrix and $\boldsymbol{\Lambda}_0 \in \mathbb{R}^{M\times N}$ with an all-one matrix. *Example 1*: First, we study how the regularization factor γ, step parameter η and step size μ, affect the mean square error (MSE) performance [21] of the estimated matrix $\hat{\boldsymbol{X}}$ for the proposed method, respectively. In general, the MSE curves versus the tunable parameters, i.e., γ, η and μ are depicted in Fig. 2, where it is obvious that the MSE can be regarded as convex function with respect to these tunable parameters. Therefore, a set of tunable parameters can be found to minimize the MSE. Specifically, the MSE gets the minimum value, about 1.4×10^{-3}, in the case of $\gamma = 5$, $\eta = 0.1$ and $\mu = 0.01$. Therefore, these parameter values are selected in the following tests unless specified otherwise. Furthermore, according to the theory of satellite signal acquisition [2], we assume that the navigation receiver can work normally, if the MSE of the recovered satellite signal matrix $\hat{\boldsymbol{X}}$ is less than or equal to 5×10^{-3}. As a result, the approximate applicable ranges of the tunable parameters γ, η and μ are [0.7, 14.5], [0.06, 0.7] and [0.0015, 0.066], respectively.

Example 2: After that, in order to analyze the convergence process of MSE with respect to the step parameters η and μ, the MSE curves versus the number of iterations are depicted in Fig. 3 and Fig. 4, respectively. In general, as the number of iterations increases, all the MSE curves can gradually decrease, which can prove that the MSE of proposed algorithm can converge. In addition, it is obvious that the parameters, η and μ, determine the convergence rate and steady-state values of these MSE curves. This is because μ and η directly affect the update rate and accuracy in (24) and (28), respectively. Furthermore, for an iterative technique, with the increase of step size, the convergence rate can be accelerated while the accuracy of convergence steady state may become worse. That is why the convergence rate of the cases, $\eta = 0.5, 0.6$, is obviously faster than that of other tested cases, while the convergence steady-state values of $\eta = 0.5, 0.6$, are slightly higher than those in other tested cases in Fig. 3. Moreover, according to our test, if the parameter η is further increased, the convergence rate will not be significantly improved, however, the steady-state value will gradually increase, which is consistent with the conclusion in Fig. 2 (b). Similarly, in Fig. 4, the MSE curve has the best convergence steady-state value in the case of $\mu = 0.01$ and the steady state will get worse if we keep increasing μ.

Example 3: Then, we compare the MSE performance of the proposed LDA-$\ell_{1,1}$ method with some existing algorithms,

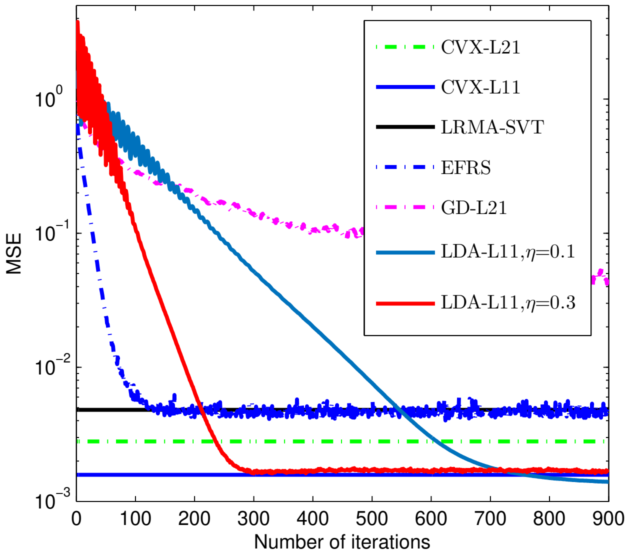

Fig. 5. MSE performance comparison, γ=5, μ=0.01.

namely, CVX-$\ell_{2,1}$, CVX-$\ell_{1,1}$, LRMA-SVT [7], EFRS [14] and direct gradient (DG)-$\ell_{2,1}$ [22]. The MSE performance versus the number of iterations is shown in Fig. 5. It is obvious that the MSE curves of the CVX-$\ell_{2,1}$, CVX-$\ell_{1,1}$, and LRMA-SVT methods do not change as the number of iterations increases, because the CVX tool [16] is directly used to calculate their optimal solutions. Furthermore, the CVX-$\ell_{1,1}$ method has lower convergence steady-state value than that of the CVX-$\ell_{2,1}$ method, because $\ell_{1,1}$-norm has more excellent ability in suppressing impulsive noise than that of $\ell_{2,1}$-norm. On the other hand, with the number of iterations increases, the MSE curves of the EFRS and LDA-$\ell_{1,1}$ methods decrease significantly while that of the DG-$\ell_{2,1}$ converges slowly. Interestingly, the steady-state value of the EFRS algorithm is exactly close to the solution of the LRMA-SVT method, and the steady state of the LDA-$\ell_{1,1}$ algorithm just approximates the solution of the CVX-$\ell_{1,1}$ method.

In addition, compared with the CVX-$\ell_{2,1}$, CVX-$\ell_{1,1}$, and LRMA-SVT methods, the EFRS and LDA-$\ell_{1,1}$ algorithms have iterative closed-form solutions, and the time consumption is much less than that of the CVX-based techniques. Furthermore, the EFRS method has the fastest convergence rate, while its MSE curve converges approximately to a higher steady-state value compared with the LDA-$\ell_{1,1}$ algorithm. It implies that the EFRS method may only suppress part of impulsive noise while the LDA-$\ell_{1,1}$ algorithm has excellent ability in terms of impulsive noise suppression. Furthermore, for the LDA-$\ell_{1,1}$ method, the parameters γ, η and μ can be flexibly adjusted to satisfy the trade-off requirement between the convergence rate and steady state.

V. Conclution

Considering the impulsive noise present environment and the spatial sparsity of satellite signals, the JANE of visible satellites was formulated as a joint $\ell_{1,1}$-norms optimization problem. In order to avoid using CVX tool and reduce the computational complexity, a dual Lagrangian multiplier algorithm with dual ascent framework was devised where a generalized conjugate function for complex-valued matrix variable was applied. Moreover, a subgradient iteration framework was employed to find a closed-form solution. Numerical results have confirmed the effectiveness of the proposed methods.

References

[1] E. Kaplan, Unstanding GPS: Principles and Applications, Second Edition, Artech House, Inc., 2006.

[2] G. Xie, Principles of GPS and receiver design. Beijing: Publishing House of Electronics Industry, 2009.

[3] S. Kong, "A deterministic compressed GNSS acquisition technique," *IEEE Trans. Veh. Technol.*, vol. 62, no. 2, pp. 511-521, Feb. 2013.

[4] M. G. Amin and Wei Sun, "A novel interference suppression scheme for global navigation satellite systems using antenna array," *IEEE J. Sel. Area. Commun.*, vol. 23, no. 5, pp. 999-1012, May 2005.

[5] D. L. Donoho, "Compressed sensing," *IEEE Trans. Inf. Theory* , vol. 52, no. 4, pp. 1289-1306, Apr. 2006.

[6] J. F. Cai, E. J. Candès and Z. Shen, " A singular value thresholding algorithm for matrix completion," *SIAM J. Optim.*, vol. 20, no. 4, pp. 1-26, Sep. 2008.

[7] A. Parekh and I. W. Selesnick, "Enhanced low-rank matrix approximation," *IEEE Signal Process. Lett.*, vol. 23, no. 4, pp. 493-497, Apr. 2016.

[8] D. L. Donoho, "De-noising by soft-thresholding," *IEEE Trans. Inf. Theory*, vol. 41, no. 3, pp. 613-627, Mar. 1995.

[9] J. Kim, J. Wang and B. Shim, "Optimal restricted isometry condition of normalized sampling matrices for exact sparse recovery with orthogonal least squares," *IEEE Trans. Signal Process.*, vol. 69, pp. 1521-1536, Feb. 2021.

[10] X. Zhang, Y. Liu and W. Cui, "Spectrally sparse signal recovery via Hankel matrix completion with prior information," *IEEE Trans. Signal Process.*, vol. 69, pp. 2174-2187, Mar. 2021.

[11] J. Li, F. Chen, Y. Wang, P. Charge, F. Ji and H. Yu, "Spatial spectrum estimation of incoherently distributed sources based on low-rank matrix recovery," *IEEE Trans. Veh. Technol.*, vol. 69, no. 6, pp. 6333-6347, Jun. 2020.

[12] Y. Chen, H. Xu, C. Caramanis and S. Sanghavi, "Matrix completion with column manipulation: Near-optimal sample-robustness-rank tradeoffs,", *IEEE Trans. Inf. Theory*, vol. 62, no. 1, pp.503-526, Jan. 2016.

[13] C. Ding, D. Zhou, X. He and H. Zha. "R1-PCA : rotational invariant ℓ_1-norm principal component analysis for robust subspace factorization," in *Pro. 23th Conf. Machine Learning*, Pittsburgh. pp. 281-288, Jun. 2006.

[14] F. Nie, H. Huang, X. Cai and C. H. Ding, "Efficient and robust feature selection via joint $\ell_{2,1}$-norms minimization," in *Proc. 23th Conf. Advance Neural Inf. Process. Syst.*, Vancouver, British Columbia, Canada, pp. 1813-1821, Dec. 2010.

[15] W. Zeng and H. C. So, "Outlier-robust matrix completion via ℓ_p-minimization," *IEEE Trans. Signal Process.*, vol. 66, no. 5, pp. 1125-1140, Mar. 2018.

[16] M. Grant and S. Boyd, CVX: Matlab software for disciplined convex programming version 2.1, build 1110, Jun. 2015. [Online]. Available: http://cvxr.com/cvx

[17] S. Boyd and L. Vandenberghe, Convex Optimization, U.K., Cambridge: Cambridge Univ. Press, 2004.

[18] H. Lütkepohl, Handbook of Matrices. New York: John Wiley & Sons, 1996.

[19] Navigation Center of United States Coast Guard and U.S. Department of Homeland Security, GPS NANUS, Almanacs, OPS Advisories, & SOF. [Online]. Available: https://navcen.uscg.gov

[20] K. Borre, D. M. Akos and N. Bertelsen, "A Software-Defined GPS and Galileo Receiver," Springer-Verlag, Berlin, Nov. 2006.

[21] C. Qian, X. Fu, N. D. Sidiropoulos, L. Huang and J. Xie, "Inexact alternating optimization for phase retrieval in the presence of outliers," *IEEE Trans. Signal Process.*, vol. 65, no. 22, pp. 6069-6082, Nov. 2017.

[22] Q. Li, L. Huang, L. Zhang, M. Huang, B. Zhao and P. Zhang, "Fast signal retrieval of sonar in the presence of impulse noise," in *Proc. 11th Sensor Array and Multichannel Signal Process. Workshop (SAM)*, Hangzhou, China, pp. 1-5, Jun. 2020.